Size dependence in tunneling spectra of PbSe quantum-dot arrays



2009 Nanotechnology 20 285401

(http://iopscience.iop.org/0957-4484/20/28/285401)

Nanotechnology **20** (2009) 285401 (5pp) doi:10.1088/0957-4484/20/28/285401

# Size dependence in tunneling spectra of PbSe quantum-dot arrays

**Y C Ou[1], S F Cheng[2] and W B Jian[2]**

[1] Institute of Physics, National Chiao Tung University, Hsinchu 30010, Taiwan
[2] Department of Electrophysics, National Chiao Tung University, Hsinchu 30010, Taiwan

E-mail: wbjian@mail.nctu.edu.tw

Received 1 February 2009, in final form 4 May 2009
Published 23 June 2009
Online at stacks.iop.org/Nano/20/285401

**Abstract**
Interdot Coulomb interactions and collective Coulomb blockade were theoretically argued to be a newly important topic, and experimentally identified in semiconductor quantum dots, formed in the gate confined two-dimensional electron gas system. Developments of cluster science and colloidal synthesis accelerated the studies of electron transport in colloidal nanocrystal or quantum-dot solids. To study the interdot coupling, various sizes of two-dimensional arrays of colloidal PbSe quantum dots are self-assembled on flat gold surfaces for scanning tunneling microscopy and scanning tunneling spectroscopy measurements at both room and liquid-nitrogen temperatures. The tip-to-array, array-to-substrate, and interdot capacitances are evaluated and the tunneling spectra of quantum-dot arrays are analyzed by the theory of collective Coulomb blockade. The current–voltage of PbSe quantum-dot arrays conforms properly to a scaling power law function. In this study, the dependence of tunneling spectra on the sizes (numbers of quantum dots) of arrays is reported and the capacitive coupling between quantum dots in the arrays is explored.

(Some figures in this article are in colour only in the electronic version)

## 1. Introduction

With the help of the semiconductor technology, including epitaxial growth and lithography techniques, to explore the system of a two-dimensional electron gas (2DEG) in the past three decades, atom-like semiconductor quantum dots (QDs) have been fabricated and measured to reveal single electron changing and artificial-atom states [1, 2]. Although the quantum size, quantum confinement, effect was proposed [3, 4] and experimentally established with the aid of developments in cluster science and physical growth [5], making crystalline particles was more recently achieved by a chemical synthesis [6] for studies of the fundamental properties of small-size objects. Colloidal synthesis with size-selective sieves is an advantageous way to manipulate the composition, size, shape, and internal structure of a large quantity of monodispersed nanocrystals or semiconductor QDs [7]. A narrow size distribution facilitates the observation of the effects of size on the optical and magnetic properties, and self-assembly to form QD films and solids. In addition, Coulomb blockade (single electron charging) and artificial-atom states have been discovered in a single crystalline metal cluster [8, 9] or semiconductor QD [10–12] using scanning tunneling microscopy (STM). As for 2DEG QDs in which interdot Coulomb interactions and tunnelings can be regulated by gate voltage [13, 14], interdot coupling in colloidal QDs, derived from organic molecules, has been adjusted through pressure and removal of capping ligands [15, 16]. The study of changes in the electrical and optical properties due to interdot coupling can support the tailoring of functional colloidal QD solids.

At low enough temperatures, a single QD manifests itself in current–voltage ($I$–$V$) in either the Coulomb blockade or the atom-like region, or both. The self-assembled QDs, QD solids or films, may expose collective behavior of either the Coulomb blockade or the artificial-atom states when the interdot coupling is taken into consideration. On the other hand, QD solids or films at a high temperature, at which quantum effects are totally destroyed by thermal fluctuation, could exhibit either an electron hopping or a thermally activated transport [17, 18]. The collective behavior of electrons in the Coulomb blockade region has been experimentally demonstrated in systems of 2DEG QD [19], and of metal island [20], arrays. In addition, Middleton and Wingreen [21]

 

proposed a model (MW model) to describe collective transport in arrays of small metallic dots in the Coulomb blockade region. They suggested a stray field to induce different polarization charges in QDs and to render a quenched disorder. The disorder leads to a threshold voltage $V_{th}$ below which the current is suppressed. At voltages well above $V_{th}$, they predicted that the current through the QD array will behave as a power law function of a reduced voltage $(V/V_{th} - 1)$ with a scaling exponent $\zeta$. They calculated the dependence of $V_{th}$ and $\zeta$ on the dimension of, and the interdot coupling in, the array. Recently, collective transport in the Coulomb blockade region has been experimentally inspected in quasi-one-dimensional wires [22, 23], two-dimensional films [24, 25], and three-dimensional solids [26, 27] self-assembled by colloidal QDs.

In our previous study, we have analyzed $I$–$V$'s of PbSe QD arrays based on the semiclassical orthodox theory [28]. Here, we report the size dependent tunneling spectra of self-assembled PbSe QD arrays using STM and current image tunneling spectra (CITS) at both room and liquid-nitrogen temperatures. We adopted the MW model to analyze the tunneling spectra of colloidal QD arrays. To deviate from the parallel array, in which the current is parallel to one of its two dimensions, as proposed in the MW model, we will study the electron transport of perpendicular arrays, having a current flow perpendicular to both the two dimensions of the arrays.

## 2. Experimental details

A high-temperature organic solution approach and a size-selection procedure were employed in the synthesis of colloidal PbSe QDs [7, 28, 29]. The as-synthesized QDs, capped with both oleic acid and trioctylphosphine (TOP), were scrutinized by a transmission electron microscope (JEOL JEM-2010F) to check their shapes, structures, and sizes [29]. The PbSe QDs appear as a single crystalline structure with either a spherical or cubic shape. Their sizes possess a narrow distribution with an average diameter of 14.6 nm and a standard deviation of 17%. After material characterizations, PbSe QDs were dispersed in the toluene solvent using ultrasonic vibration. Several drops of the dilute QD solution were deposited on a flat gold surface which was prepared by melting a 2 mm diameter gold wire and by quenching in air. Through adjusting the self-assembly conditions, such as the substrate temperature and the concentration of QD solution [30], different sizes of two-dimensional islands made of PbSe QDs can be formed on the gold substrate after the toluene solvent has evaporated. The self-assembling behavior was checked with an atomic force microscope (Seiko Instruments Inc. SPA-300HV) and a field-emission scanning electron microscope (JEOL JSM-7000F). The as-prepared sample containing QD islands was loaded into a preparation chamber of a low-temperature STM (Omicron LTSTM) and annealed overnight at 150 °C in an ultrahigh vacuum of $\sim 1 \times 10^{-10}$ Torr. Subsequently, the sample was transferred to the main chamber for performing the STM measurements. An electrochemically etched tungsten tip was used in our experiment. All STM topography images of QD arrays were carried out in a constant current mode with the scanning parameters of a sample bias voltage $V_s = 2.5$ V and a set-point tunneling current $I_t = 0.15$ nA. CITS data ramped from 1.5 to −1.5 V with 200 steps were acquired with the bias voltage turned down to $V_s = 1.5$ V. The STM images and CITS data were recorded at both room temperatures and 78 K. A characteristic $I$–$V$ of a PbSe QD array is an average of several thousands of CITS data. The $I$–$V$ was analyzed and fitted by the Levenberg–Marquardt nonlinear least squares method [31].

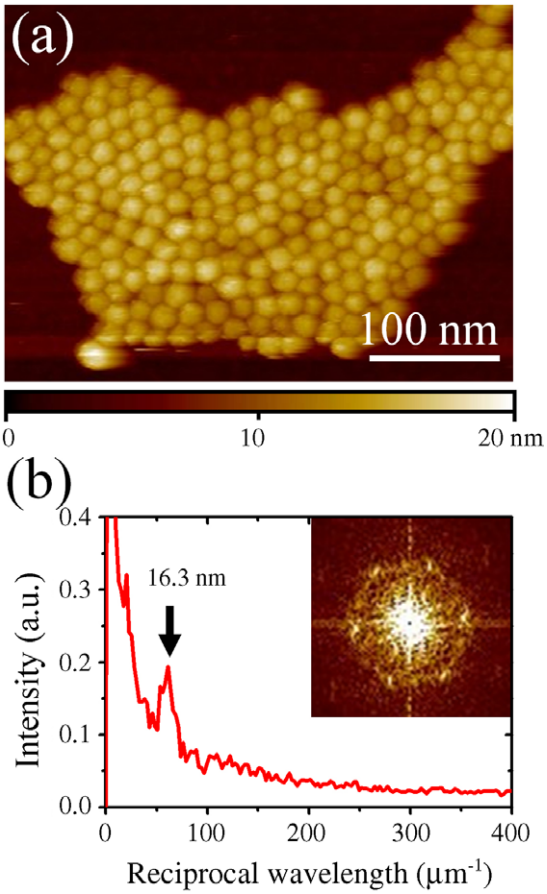


**Figure 1.** (a) STM image of a typical PbSe QD array on a flat Au(111) surface. (b) Radially averaged intensity of the two-dimensional Fourier transformed image displayed in the inset. The peak marks a periodical length of ∼16.3 nm for the distance between centers of two neighboring PbSe QDs.

## 3. Results and discussion

Before annealing in an ultrahigh vacuum, PbSe QDs form a monolayer of two-dimensional islands demonstrating either disordered clusters or locally regular arrangements. The as-deposited QD islands seem to be mobile and cause a blurred image under the scanning measurements of STM. After annealing and removal of excess capping agents, the QD islands are organized as two-dimensional arrays and fixed on a flat gold surface to stabilize the STM scans. Figure 1(a) shows a two-dimensional PbSe QD array with 229 QDs on the Au(111) surface. The arrays appear as a hexagonal or, sometimes, a square lattice in two dimensions and have a rounded shape. The average number of nearest neighbors of the PbSe QD in the arrays is about 6. In order

to distinguish either electron tunneling or direct contact in forming conduction channels among PbSe QDs, the separation distance between the QDs is estimated: the STM topography image is transformed to a two-dimensional Fourier image like that shown in the inset of figure 1(b); the radially average intensity of the fast Fourier transform image is calculated and displayed in figure 1(b) to give a peak which indicates a spacial periodicity of ∼16.3 nm between the centers of two PbSe QDs. In particular, the fast Fourier transform image in the inset of figure 1(b) clearly exhibits 6 dots, symptomatic of a hexagonal lattice. Since the average diameter of the PbSe QDs is 14.6 nm, the separation distance between two PbSe QDs is evaluated to be 1.7 nm, which is about two layers of organic molecules of the TOP and oleic acid. Using a parallel plate capacitor model with the interdot spacing 1.7 nm and taking the QDs as cubic with one side 14.6 nm, we can judge the interdot capacitance to be about 2.26 aF. The interdot capacitance gives a Coulomb charging energy of 35.4 meV, which is still higher than the room-temperature thermal energy of ∼25 meV, so the interdot coupling should be observable. On the other hand, the STM tip-to-array and the array-to-substrate capacitances are evaluated to be about 0.05 and 0.08 aF, respectively, according to the double-barrier tunnel-junction model [28]. The small value of the tip-to-array and array-to-substrate capacitances result in a high Coulomb charging energy and points to a collective Coulomb blockade region for our system, PbSe QD arrays, even at room temperatures. In addition, the QD diameter is comparatively large. We have only observed artificial-atom states on $I$–$V$'s at 5 K, so we believe that the PbSe QDs are still in a Coulomb blockade region at both room temperatures and 78 K.

Figure 2(a) presents the characteristic tunneling spectrum ($I$–$V$) of a PbSe QD array consisting of 43 QDs on a flat gold surface at room temperatures. The characteristic $I$–$V$ reveals a symmetric feature about zero voltage and contains a zero-current, Coulomb blockade voltage range, a threshold voltage $V_{\rm th}$ above which the current starts to flow across the QD array, and a high voltage range with a large current implying, open conduction channels. The characteristic $I$–$V$ is symmetric so only the current in the positive voltage range is analyzed based on the scaling power law $I \propto (V - V_{\rm th})^{\zeta}$ of the MW model. Figure 2(b) shows experimental data (open circles) and a nonlinear least square fitting curve (a solid line) to demonstrate that our $I$–$V$ data are in concordance with the scaling law proposed in the MW model. The parameters, the threshold voltage $V_{\rm th}$ and scaling exponent $\zeta$, can be estimated after fitting. The threshold voltage $V_{\rm th} = 0.49$ V seems to be in line with a Coulomb blocking voltage from the tip-to-array and array-to-substrate capacitances. Furthermore, the estimated scaling exponent $\zeta = 2.31$ is in the range of those obtained from two-dimensional arrays [24, 25], which give $\zeta$ between 2.2 and 2.7, and it is smaller than those evaluated from three-dimensional [26, 27] arrays ($2.5 < \zeta < 4.5$). Figure 2(c) illustrates how an electron transports from the STM tip to the flat gold surface and through a PbSe QD array. The polarization, residual charges on QDs could be different so as to render a quenched disorder of polarization charges in the array. As an electron tunnels from the STM

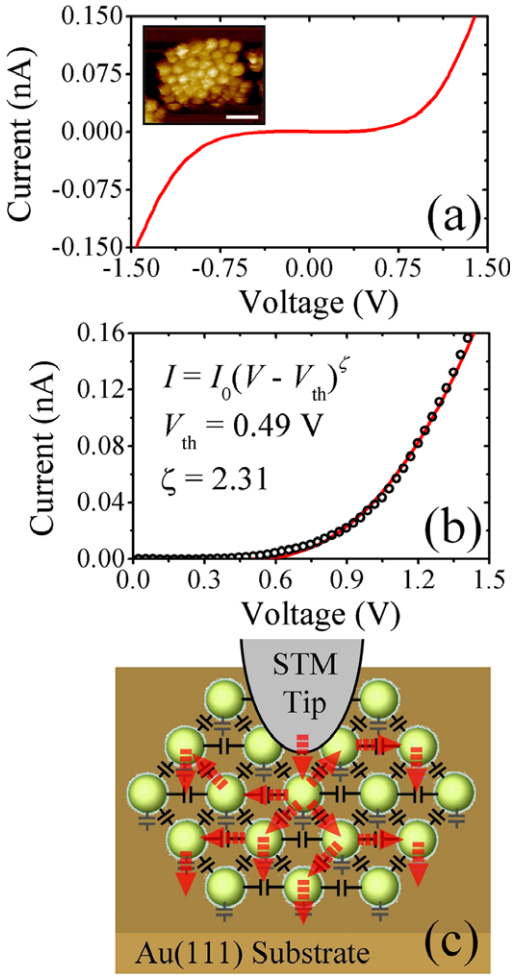


**Figure 2.** (a) The $I$–$V$ curve of an array consisting of 43 PbSe QDs. The inset displays its STM topography image with a 50 nm scale bar. (b) Experimental data (open circles) and a fitting curve (solid line) according to the indicative power law function. The nonlinear least square fitting gives the parameters of the threshold voltage and the scaling exponent designated in the inset. (c) Schematic illustration of the model of collective transport. The spheres denote PbSe QDs. The black and gray thin lines indicate the interdot and dot-to-substrate capacitances, respectively. The dashed thick lines with arrows illustrate electron transport.

tip to the QD array, it will tunnel to a QD having far less polarization charge in order to reduce the Coulomb charging energy. In addition, as compared with the tip-to-array and array-to-substrate capacitances, the interdot capacitance is two orders of magnitude larger to have a smaller Coulomb charging energy. The electron could tunnel to a nearest neighbor QD to reduce the high Coulomb charging energy in the PbSe QD situated in between the STM tip and the gold substrate. As pointed out in the MW model [21], a comparatively large interdot capacitance gives rise to a long screening length in the QD array and a decrease in the threshold voltage $V_{\rm th}$ per QD. When the bias voltage is higher than $V_{\rm th}$, the electron will find the best way, shunting high charging energy, to transport between the STM tip and the substrate. When more and more current paths are opened with an increasing bias voltage, the $I$–$V$ will follow the proposed power law function. In

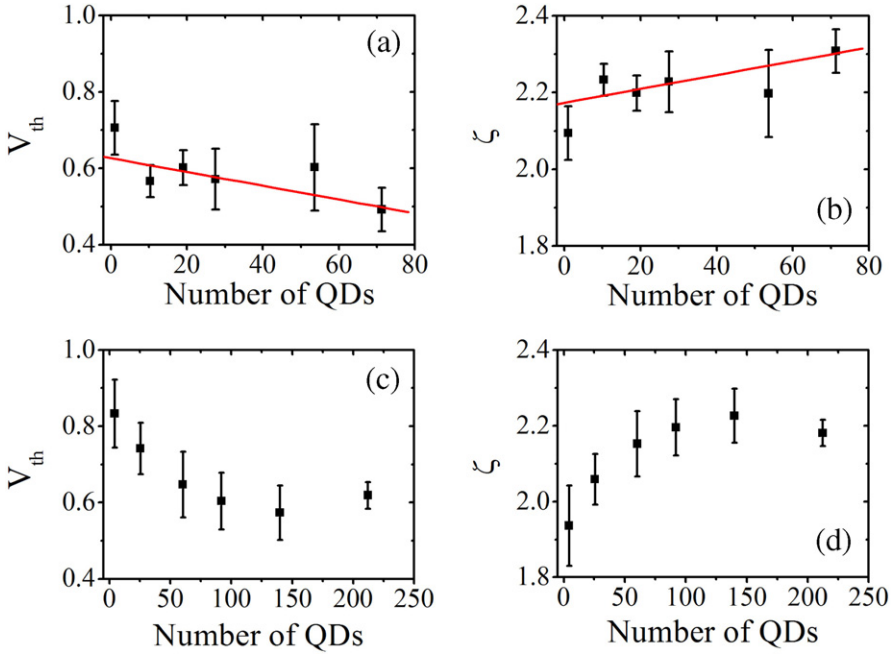


**Figure 3.** Threshold voltages $V_{th}$ ((a) and (c)) and scaling exponents $\zeta$ ((b) and (d)) as a function of the QD number. The data in (a) and (b) ((c) and (d)) are estimated from fitting to $I$–$V$ curves taken at room temperature (78 K). The solid lines in (a) and (b) give the best linear least square fits to our data.

the following paragraph, we will see the size dependence of $V_{th}$ and the scaling exponent $\zeta$ after the onset of a tunneling current.

Characteristic $I$–$V$'s of PbSe QD arrays with various numbers of QDs were obtained at both room temperature and 78 K, and the data were fitted with the power law function $I \propto (V - V_{th})^{\zeta}$ to extract the $V_{th}$ and $\zeta$. Figures 3(a) and (b) show the $V_{th}$ and $\zeta$ dependences on the array size as well as the number of QDs at room temperatures. As the QD number of the array rises from 1 to 80, the threshold voltage $V_{th}$ gradually decreases and the scaling exponent $\zeta$ goes up slightly. A large interdot capacitance implies a strong coupling between the QDs and a long screening length in the PbSe QD array, so the addition of extra QDs could be used to examine the reduction in $V_{th}$ due to the interdot capacitive coupling. From about 0.7 V for a single QD, the $V_{th}$ drops to 0.5 V for an array containing 71 PbSe QDs. Meanwhile, $\zeta$ goes up in value from about 2.1 to 2.3, suggesting more current paths opened in a high bias voltage with the addition of PbSe QDs into the array. The dependence of both $V_{th}$ and $\zeta$ on the array size seems to be in line with the theoretical arguments of the MW model. In addition, the $V_{th}$ and $\zeta$ estimated at room temperature are scattered and we thus repeat our experiments at 78 K and display the $V_{th}$ and $\zeta$ in figures 3(c) and (d), respectively. The scattering in the $V_{th}$ and $\zeta$ is, in particular, abated for data taken at 78 K due to the reduced thermal fluctuation. Before we go ahead to discuss the low-temperature data, we should address the quantitative validity of our data. Figures 3(a) and (b) present a rather large standard deviation in $V_{th}$ and $\zeta$ and, thus, the least square fitting line can only give a rough tendency. The data shown in figures 3(c) and (d), however, demonstrate a noticeable decrease and an increase in the $V_{th}$ and $\zeta$, respectively. The variation trend, which is in agreement with the room-temperature data, is much clearer since the change in the $V_{th}$ and $\zeta$ as a function of a QD number is larger than the value of the standard deviations. We consequently confirm that our data can give a quantitative validity to examine the theoretical model. Additionally, it is noteworthy that the $V_{th}$ and $\zeta$ at 78 K still reveal appreciable error bars, possibly resulting from the size distribution of PbSe QDs.

The single QD $V_{th}$ and $\zeta$ taken at 78 K shift to about 0.8 V and 1.9 (figures 3(c) and (d)) in comparison with $V_{th} = 0.7$ V and $\zeta = 2.1$ at room temperatures (figures 3(a) and (b)). We believe that a small thermal fluctuation helps to widen the Coulomb blocking voltage ($V_{th}$) and to reduce the thermally excited current paths ($\zeta$). For the data taken at 78 K, the $V_{th}$ decrease from 0.8 to 0.6 V while the $\zeta$ increase from 1.9 to 2.2 when the QD number of the array increases from 1 to 220. The size dependency at 78 K conforms to that observed at room temperature when the QD number of the array is less than 100. In addition to the change in the $V_{th}$ and $\zeta$ as a function of the QD number, we notice, as well, a saturation trend in both the $V_{th}$ and $\zeta$ for PbSe QD arrays containing a number of QDs larger than 100. The result seems to agree well with the theoretical argument of a strong interdot coupling, resulting in a long capacitive screening length. When the QD number or size of the array is comparatively larger than the screening length, the collective Coulomb blockade effect will not be altered further and both the $V_{th}$ and $\zeta$ will reach saturated values. The limit of collective transport appearing in a finite screening length is revealed for the first time.

## 4. Conclusions

Using the low-temperature STM, tunneling spectra of various sizes of two-dimensional self-assembled PbSe QD arrays have

been measured on flat gold surfaces at both room temperature and 78 K. Estimated from the Fourier transformed STM image, the interdot capacitance between the PbSe QDs is two orders of magnitude larger than both the tip-to-array and array-to-substrate capacitances, leading to a strong interdot coupling and a long screening length. The characteristic $I$–$V$ of the QD array is analyzed in accordance with the collective Coulomb blockade effect and fitted with the scaling power law $I \propto (V - V_{\mathrm{th}})^{\zeta}$ of the Middleton–Wingreen model to extract threshold voltages $V_{\mathrm{th}}$ and the scaling exponents $\zeta$. The size dependence of the threshold voltage $V_{\mathrm{th}}$ and the scaling exponent $\zeta$ demonstrates a drop in $V_{\mathrm{th}}$ and a rise in $\zeta$ when the QD number increases from 1 to 80. Meanwhile, a saturation tendency for arrays with QD numbers greater than 100 has been perceived both in $V_{\mathrm{th}}$ and $\zeta$ for data acquired at 78 K. An enhancement in the collective behavior of interdot couplings through the addition of PbSe QDs has been explored. Additionally, a decrease in the Coulomb blocking voltage ($V_{\mathrm{th}}$) and an increase in conduction channels ($\zeta$) in the PbSe QD arrays have been experimentally established to be consistent with the theoretical model.

## Acknowledgments

The authors thank Professor Jiye Fang for providing quantum-dot materials and Professor Juhn-Jong Lin for using his facilities. This work was supported by the Taiwan National Science Council under Grant No. NSC 95-2112-M-009-045-MY3 and by the MOE ATU Program.

## References

[1] Kastner M A 1992 *Rev. Mod. Phys.* **64** 849
[2] Reimann S M and Manninen M 2002 *Rev. Mod. Phys.* **74** 1283
[3] Kubo R 1962 *J. Phys. Soc. Japan* **17** 975
[4] Brus L E 1984 *J. Chem. Phys.* **80** 4403
[5] Phillips J C 1986 *Chem. Rev.* **86** 619
[6] Alivisatos A P 1996 *Science* **271** 933
[7] Murray C B, Sun S, Gaschler W, Doyle H, Betley T A and Kagan C R 2001 *IBM J. Res. Dev.* **45** 47
[8] Wilkins R, Ben-Jacob E and Jaklevic R C 1989 *Phys. Rev. Lett.* **63** 801
[9] Andres R P, Bein T, Dorogi M, Feng S, Henderson J I, Kubiak C P, Mahoney W, Osifchin R G and Reifenberger R 1996 *Science* **272** 1323
[10] Banin U, Cao Y, Katz D and Millo O 1999 *Nature* **400** 542
[11] Katz D, Millo O, Kan S H and Banin U 2001 *Appl. Phys. Lett.* **79** 117
[12] Bakkers E P A M, Hens Z, Zunger A, Franceschetti A, Kouwenhoven L P, Gurevich L and Vanmaekelbergh D 2001 *Nano Lett.* **1** 551
[13] Waugh F R, Berry M J, Mar D J, Westervelt R M, Campman K L and Gossard A C 1995 *Phys. Rev. Lett.* **75** 705
[14] Stafford C A and Das Sarma S 1994 *Phys. Rev. Lett.* **72** 3590
[15] Collier C P, Saykally R J, Shiang J J, Henrichs S E and Heath J R 1997 *Science* **277** 1978
[16] Kim D I, Islam M A, Avila L and Herman I P 2003 *J. Phys. Chem.* B **107** 6318
[17] Kim S H, Medeiros-Ribeiro G, Ohlberg D A A, Williams R S and Heath J R 1999 *J. Phys. Chem.* B **103** 10341
[18] Mentzel T S, Porter V J, Geyer S, MacLean K, Bawendi M G and Kastner M A 2008 *Phys. Rev.* B **77** 075316
[19] Duruöz C I, Clarke R M, Marcus C M and Harris J S Jr 1995 *Phys. Rev. Lett.* **74** 3237
[20] Rimberg A J, Ho T R and Clarke J 1995 *Phys. Rev. Lett.* **74** 4714
[21] Middleton A A and Wingreen N S 1993 *Phys. Rev. Lett.* **71** 3198
[22] Bezryadin A, Westervelt R M and Tinkham M 1999 *Appl. Phys. Lett.* **74** 2699
[23] Elteto K, Lin X M and Jaeger H M 2005 *Phys. Rev.* B **71** 205412
[24] Black C T, Murray C B, Sandstorm R L and Sun S 2000 *Science* **290** 1131
[25] Parthasarathy R, Lin X M and Jaeger H M 2001 *Phys. Rev. Lett.* **87** 186807
[26] Fan H, Yang K, Boye D M, Sigmon T, Malloy K J, Xu H, López G P and Brinker C J 2004 *Science* **304** 567
[27] Blunt M O, Šuvakov M, Pulizzi F, Martin C P, Pauliac-Vaujour E, Stannard A, Rushforth A W, Tadić B and Moriarty P 2007 *Nano Lett.* **7** 855
[28] Ou Y C, Wu J J, Fang J and Jian W B 2009 *J. Phys. Chem.* C **113** 7887
[29] Jian W B, Lu W, Fang J, Chiang S J, Lan M D, Wu C Y, Wu Z Y, Chen F R and Kai J J 1996 *J. Chem. Phys.* **124** 064711
[30] Ge G and Brus L E 2001 *Nano Lett.* **1** 219
[31] Press W H, Flannery B P, Teukolsky S A and Vetterling W T 1986 *Numerical Recipes* (New York: Cambridge University Press) p 523